Monthly Notices
of the
ROYAL ASTRONOMICAL SOCIETY

MNRAS **436,** 315–326 (2013)
Advance Access publication 2013 September 11

doi:10.1093/mnras/stt1567

The most luminous quasars do not live in the most massive dark matter haloes at any redshift

N. Fanidakis,[1]⋆ A. V. Macciò,[1] C. M. Baugh,[2] C. G. Lacey[2] and C. S. Frenk[2]

[1]*Max-Planck-Institute for Astronomy, Königstuhl 17, D-69117 Heidelberg, Germany*
[2]*Institute for Computational Cosmology, Department of Physics, University of Durham, Science Laboratories, South Road, Durham DH1 3LE, UK*

Accepted 2013 August 19. Received 2013 August 13; in original form 2013 May 7

ABSTRACT

Quasars (QSOs) represent the brightest active galactic nuclei (AGN) in the Universe and are thought to indicate the location of prodigiously growing black holes (BHs), with luminosities as high as 10^{48} erg s^{-1}. It is often expected though that such an extremely energetic process takes place in the most massive bound structures in the dark matter (DM) distribution. We show that in contrast to this expectation, in a galaxy formation model which includes AGN feedback, QSOs are predicted to live in DM haloes with typical masses of a few times 10^{12} M$_\odot$. Such an environment is considered to be average in the low-redshift universe ($z \lesssim 2$–3) and almost comparable to a Milky Way halo. This fundamental prediction arises from the fact that QSO activity (i.e. BH accretion with luminosity greater than 10^{46} erg s^{-1}) is inhibited in more massive DM haloes, where AGN feedback operates. The galactic hosts of QSOs in our simulations have typical stellar masses of 10^{10}–10^{11} M$_\odot$, and represent remnants of massive disc galaxies that have undergone a disc instability or galaxy merger. Interestingly, we find no dependence of QSO activity on environment; thus, the typical QSO halo mass remains constant over two orders of magnitude in luminosity. We further show that the $z \sim 6$ QSOs do not inhabit the largest DM haloes at that time as these environments are already subject to feedback. Their descendants at $z = 0$ span a wide range of morphologies and galaxy masses, and their BHs typically grow only by a modest factor between $z \sim 6$ and the present day. We predict that there should be an enhancement in the abundance of galaxies around QSOs at $z \sim 5$. However, these enhancements are considerably weaker compared to the overdensities expected at the extreme peaks of the DM distribution. Given that high-z QSO descendants are typically found in rich clusters ($\sim 10^{14}$ M$_\odot$) and very seldom in the most massive haloes, we conclude that it is very unlikely that QSOs observed at $z \gtrsim 5$ trace the progenitors of today's superclusters.

Key words: galaxies: haloes – cosmology: theory – dark matter – large-scale structure of Universe.

1 INTRODUCTION

The clustering of dark matter (DM) haloes is a well-studied problem, since it is exclusively determined by the nature of the DM particle, gravity and the expansion history of the Universe. Numerical simulations and analytical models show that there is a strong dependence of clustering on mass, with higher mass haloes being more clustered than lower mass haloes (Sheth & Tormen 1999). On the other hand, the clustering of galaxies depends strongly on the physics of galaxy formation [gas cooling, star formation (SF), feedback] and does not exactly map the distribution of DM. As a consequence, galaxies are biased tracers of the DM distribution (Kaiser 1984; Bardeen et al. 1986; Cole & Kaiser 1989; Mo & White 1996). However, despite its complexity, there is a strong dependence of galaxy clustering on luminosity, which implies that more luminous galaxies live in more massive haloes than less luminous galaxies (Norberg et al. 2001; Zehavi et al. 2005). In this context, quasars (QSOs) have gained immense popularity as galaxy tracers of the most massive haloes at high redshifts, because they are extremely bright and are observed at great distances. Consequently, if QSOs live in the most massive haloes, it is expected that those detected at high redshifts should directly probe the early growth of these structures. Yet, it remains unclear whether or not bright QSOs do indeed reside in the extremes of the DM distribution.

In the low-z Universe ($z \lesssim 2$), clustering studies of QSOs in large surveys such as the Sloan Digital Sky Survey (SDSS) and the Two-degree Field (2dF) suggest that the typical DM halo mass of

⋆ E-mail: fanidakis@mpia.de

luminous QSOs is (2–3) $\times$ $10^{12}\,h^{-1}\,M_{\odot}$ (Porciani, Magliocchetti & Norberg 2004; Wake et al. 2004; Croom et al. 2005; Ross et al. 2009, see also Shanks et al. 2011). This is considerably lower than the mass of the largest haloes in place at that redshift (which typically is of the order of 10^{14}–$10^{15}\,M_{\odot}$) and independent of QSO luminosity (see however Shen et al. 2012). Therefore, QSOs in the low-z Universe reside in average regions of the DM distribution. This picture is supported by semi-analytical studies, in which QSO activity is usually driven by galaxy–galaxy mergers (Enoki, Nagashima & Gouda 2003; Bonoli et al. 2009, 2010, see also Marulli et al. 2008). The model by Bonoli et al. (2009), which is built upon the galaxy formation model of De Lucia & Blaizot (2007), predicts an average halo mass of 10^{12}–$10^{13}\,M_{\odot}$ for QSOs. QSO activity in more massive haloes is typically inhibited due to the suppression of gas cooling by active galactic nucleus (AGN) feedback.

In the high-z Universe ($z \gtrsim 2$) the picture is not clear. The clustering of $z \geq 2.9$ QSOs in the SDSS indicates a minimum halo mass of (3–6) $\times$ $10^{12}\,h^{-1}\,M_{\odot}$, slightly more massive than that of their lower-z counterparts (Shen et al. 2007). The strong clustering of QSOs in their sample implies that QSOs in the high-z Universe are tracers of highly biased massive haloes. These predictions sparked numerous studies of the environment of high-z QSOs. In these studies, the environment of QSOs is usually probed by estimating the abundance of emission line galaxies such as Hα galaxies, Lyα emitters (LAEs) or Lyman break galaxies (LBGs) around the QSO. A higher abundance of galaxies compared to the field typically indicates an overdensity, which then implies that the host halo is relatively overmassive. At such high redshifts, these structures could be collapsing and forming today's clusters, and therefore, it is likely that the QSO under investigation pinpoints the direct location of a protocluster. Interestingly, there is an ambiguity regarding the conclusions of the different observational studies in the literature. Even though a certain number of studies suggest that QSOs indeed trace massive structures (Cantalupo, Lilly & Haehnelt 2012; Swinbank et al. 2012), an equal number claim that the environment of QSOs is average (Francis & Bland-Hawthorn 2004; Kashikawa et al. 2007, see also Trainor & Steidel 2012).

The quest to find overdensities around QSOs becomes of particular interest when the most distant ($z \geq 5$) QSOs are considered. The relatively high luminosities of these objects indicate that the mass of the black holes (BHs) powering accretion is close to $10^{9}\,M_{\odot}$, already at $z = 7$ (Mortlock et al. 2011). This implies that the BHs in the $z \sim 6$ QSOs have grown in environments where the existence of abundant cold gas is favoured. It is appealing then to associate these environments with the most massive structures of DM, where gas cooling is expected to be prodigious. For this reason, it has often been assumed that the most distant QSOs reside at the peaks of the DM distribution (Fan et al. 2003) and therefore trace the location of the progenitors of today's superclusters. This assumption has become the norm in theoretical studies of the evolution of the DM distribution and galaxies, where QSOs are generally associated with the most massive DM haloes in the early universe (Springel et al. 2005; Trenti, Santos & Stiavelli 2008; Capak et al. 2011; Angulo et al. 2012). Interestingly, when mock catalogues of star-forming galaxies predicted using semi-analytic models (which are usually built upon these simulations) are compared with the observations, it is found that several observed $z \sim 6$ QSO fields are not particularly overdense (Overzier et al. 2009). Yet, given that the observations of $z \sim 6$ QSO fields are incomplete, it is not possible to rule out that QSOs could be found at the extremes of the DM distribution.

Observationally, there have been several studies that support this idea, usually by probing overdensities of faint i_{775}-dropout (Stiavelli et al. 2005; Zheng et al. 2006) or sub-mm galaxies (Priddey, Ivison & Isaak 2008) in the fields of $z \sim 6$ QSOs. However, Willott et al. (2005) performed deep optical imaging of three $6.2 < z < 6.5$ QSO fields and found no evidence of i'-band dropout overdensities (see also Carilli et al. 2004). Similarly, Kim et al. (2009) observed i_{775}-dropouts in five $z \sim 6$ SDSS QSOs fields and found that only two show any evidence of an overdensity. In a more recent study, Bañados et al. (2013) searched for LBGs and LAEs in the field of a $z = 5.7$ QSO, probing LAEs in a narrow redshift range of $\Delta z \simeq 0.1$. The authors show that the LAE abundances are consistent with those found in random fields, and therefore the QSO does not reside in an overdensity. Thus, the picture emerging for the $z \geq 5$ QSOs is also not clear.

Here we present a study of the DM environment of QSOs by employing the semi-analytic model GALFORM. In this model, the formation and evolution of galaxies and BHs are fully coupled, and modelled consistently within the hierarchical clustering of the DM distribution (Fanidakis et al. 2011, 2012). The aim of the study is to shed light on the typical halo mass of QSOs in the low- and high-z Universe and to provide a physical framework within which the aforementioned observations can be explained. The paper is organized as follows. In Section 2, we briefly describe the main points of the model used in this analysis. In Section 3, we present the predictions of the model for the correlation between AGN luminosity and host halo mass, and demonstrate how QSOs inhabit average DM environments. In Section 4, we explore the environmental dependence of the brightest QSOs in the early universe and trace their descendants to $z = 0$. In the same section, we also make predictions for the expected number of galaxies around QSOs in order to understand better the observations of QSO overdensities at high z. Finally, we complete our analysis by summarizing our findings in Section 5. The cosmology adopted in our simulations is similar to the best constraints on the cosmological parameters from the analysis of the seven-year data release from the *Wilkinson Microwave Anisotropy Probe* (*WMAP*7; Komatsu et al. 2011). Throughout this paper, we choose $\Omega_{\rm m} = 0.227$, $\Omega_{\rm b} = 0.045$, $\Omega_{\Lambda} = 0.728$ and $\sigma_8 = 0.81$.[1] We set $h = 0.7$ for all galaxy properties that we calculate.

2 THE MODEL

To tackle the key questions of galaxy formation, several techniques have been devised over the past two decades. Among the most prominent is semi-analytical modelling (see Baugh 2006; Benson 2010 for a review). Semi-analytical models combine the strength of direct N-body simulations of the DM density field with the flexibility of a set of coupled differential equations that describe the physical processes that govern galaxy formation and evolution. The former approach has the advantage of being computationally inexpensive and therefore ideal for exploring the BH parameter and model (adding new physics) space. Among the most prominent semi-analytical models is GALFORM (Cole et al. 2000).

GALFORM takes into account in a self-consistent way all the main processes involved in galaxy formation: (i) formation and evolution of DM haloes in the Λ cold dark matter cosmology, (ii) gas

[1] $\Omega_{\rm m}$, $\Omega_{\rm b}$ and Ω_{Λ} express the present density of the baryonic, total matter and dark energy components of the Universe relative to the critical density ($\rho_{\rm crit} = 3H^2/8\pi G$). σ_8 measures the rms mass fluctuations in spheres of radius $8\,h^{-1}$ Mpc linearly extrapolated to the present day.

cooling and disc formation in DM haloes, (iii) SF, supernova feedback and chemical enrichment, (iv) BH growth and AGN feedback, and (v) formation of bulges during galactic disc instabilities and galaxy mergers. The model has been successful in reproducing many observations including the luminosity and stellar mass function of galaxies, the number counts of submillimetre galaxies, the evolution of LAEs and LBGs, the H I and H II mass functions and the AGN diversity and evolution (Baugh et al. 2005; Bower et al. 2006; Orsi et al. 2008; Fanidakis et al. 2011, 2012; Kim et al. 2011; Lacey et al. 2011; Lagos et al. 2011, 2012; Gonzalez-Perez et al. 2013). For the purposes of this analysis, we couple GALFORM with the AGN model described in Fanidakis et al. (2012). In the rest of this section, we will address the main points of the AGN model that are relevant to this analysis. We refer the reader to Fanidakis et al. for further details of the modelling of BH evolution and AGN properties.

In Fanidakis et al., we followed the mass accretion rate on to the BHs and the evolution of the BH mass, $M_{\rm BH}$, and spin in GALFORM allowing the calculation of a plethora of predictions related to the nature of AGN. The evolution of BHs and their host galaxies is fully coupled in the model: BHs grow during the different stages of the evolution of the host by accreting cold gas (merger/disc-instability-driven accretion: *starburst mode*) and hot gas (diffuse-halo-cooling-driven accretion: *hot-halo mode*) and by merging with other BHs. These processes build up the mass and spin of the BH, with the former correlating with the mass of the galaxy bulge in agreement with the observations (Häring & Rix 2004).

The hot-halo mode is of particular interest in our model since it is directly linked to the AGN feedback mechanism. In particular, during the accretion of gas in this mode, a fraction of the accretion luminosity is coupled directly to the gas in the host DM halo. If the available heating energy is high enough to balance the cooling luminosity of the gas, then the cooling is shut off. As a consequence, SF in the central galaxy is shut off. This allows us to reproduce the observed luminosity and stellar mass function of galaxies in the low- and high-z Universe. Interestingly, AGN feedback has important implications also for the evolution and clustering of AGN as it directly affects (and essentially regulates) the available cold-gas reservoir in their host galaxies (see Fanidakis et al. 2012, 2013).

The gas mass accreted during the starburst mode is converted into an accretion rate, $\dot{M}$, by assuming that the accretion duration is proportional to the dynamical time-scale of the host spheroid. In the hot-halo mode, the accretion rate is calculated using the timestep over which gas is accreted from the halo. The bolometric luminosity of the accretion flow, $L_{\rm bol}$, is then calculated by coupling the accretion rate with the Shakura–Sunyaev thin-disc model (Shakura & Sunyaev 1973)

$$L_{\rm bol} = \epsilon \dot{M} c^2, \tag{1}$$

for accretion rates higher than 1 per cent of the Eddington accretion rate ($\dot{m} = \dot{M}/\dot{M}_{\rm Edd} \geqslant 0.01$) or, otherwise, the advection-dominated accretion flow (ADAF) solution is adopted (Narayan & Yi 1994; Mahadevan 1997)

$$L_{\rm bol,ADAF} = 0.44 \left(\frac{\dot{m}}{0.01}\right) \epsilon \dot{M} c^2. \tag{2}$$

When the accretion becomes substantially super-Eddington ($L_{\rm bol} \geq \eta L_{\rm Edd}$), the bolometric luminosity is limited to (Shakura & Sunyaev 1973)

$$L_{\rm bol}(\geqslant \eta L_{\rm Edd}) = \eta[1 + \ln(\dot{m}/\eta)] L_{\rm Edd}, \tag{3}$$

where η is an ad hoc parameter, which we choose to be equal to 4 allowing a better reproduction of the bright end of the QSO luminosity function (LF). However, we do not restrict the accretion rate if the flow becomes super-Eddington. The luminosity output calculated via equations (1)–(3) is assumed to be constant during the accretion of gas. With these expressions for the bolometric luminosity of the accretion flow, we henceforth define an active galaxy in our simulation to be a QSO if its central engine exceeds 10^{46} erg s^{-1} in bolometric luminosity. Active galaxies with lower bolometric luminosities will be generally described as AGN.

The merger trees of DM structures in this analysis are extracted from the DM-only N-body simulation Millennium *WMAP*7 (Lacey et al., in preparation). The Millennium *WMAP*7 simulation has the same mass resolution ($8.61 \times 10^8\,{\rm M}_\odot$), particle number ($10^7$) and box size ($500\,h^{-1}$ Mpc) as the Millennium simulation (Springel et al. 2005) and differs only in the background cosmology (which is in agreement with *WMAP*7 results). To avoid resolution biases in the galaxy properties we calculate, we consider only DM haloes with masses greater than or equal to $10^{11}\,{\rm M}_\odot$. To test that DM haloes with masses lower than $10^{11}\,{\rm M}_\odot$ do not affect our predictions, we compare our findings with a simulation built on Monte Carlo generated trees. The Monte Carlo algorithm we use to generate the DM halo merger trees has been presented in Parkinson, Cole & Helly (2008). We find no difference between the predictions of the N-body and Monte Carlo-based simulations on the galaxy properties presented in this analysis.

We note that the AGN and galaxy formation model presented in this analysis is built upon a *WMAP*7 cosmology, whereas the cosmology of the original Fanidakis et al. model is that of *WMAP*1. A change in cosmology requires retuning of the model mainly due to the change in the value of σ_8 from *WMAP*1 to *WMAP*7. To this end, we have retuned the model to match key BH observables in the local Universe (BH scaling relations) and the overall evolution of AGN in the $z = 0$–6 Universe. In particular, we change the parameter $\nu_{\rm SF}$ to $0.5\,{\rm Gyr}^{-1}$ (this parameter quantifies the SF rate per unit molecular gas mass; the original value in Fanidakis et al. is $0.3\,{\rm Gyr}^{-1}$) and the parameter f_q to 15 (the proportionality factor between the accretion rate and bulge dynamical time-scale; the original value in Fanidakis et al. is 10). With these changes, the new best-fitting predictions for the AGN LFs at $0 \leq z \leq 6$ (in the optical, soft and hard X-ray, and bolometric bands) and the BH mass function at $z = 0$ vary insignificantly from the predictions in Fanidakis et al. (2012). We refer the reader to Fanidakis et al. (2013) for the predictions on the accretion properties and clustering of AGN and also to Lacey et al. (in preparation) for the overall properties of the background galaxy formation model in the *WMAP*7 cosmology. We further refer the reader to Guo et al. (2013) for a recent discussion on how the formation, evolution and clustering of galaxies vary with cosmological parameters.

3 THE ENVIRONMENT OF LUMINOUS QSOS

In this section, we show predictions for the DM halo mass of the AGN in our model and emphasize the host DM halo properties of the most luminous QSOs ($L_{\rm bol} \geq 10^{46}$ erg s^{-1}). We also calculate the effective DM halo mass of QSOs in order to provide a more statistical measure for the QSO environment, one that can be directly compared with the observations.

3.1 Distribution of AGN on the $L_{\rm bol}$-$M_{\rm Halo}$ plane

The existence of two modes of accretion in our model (i.e. starburst and hot-halo modes) leads to a complicated environmental

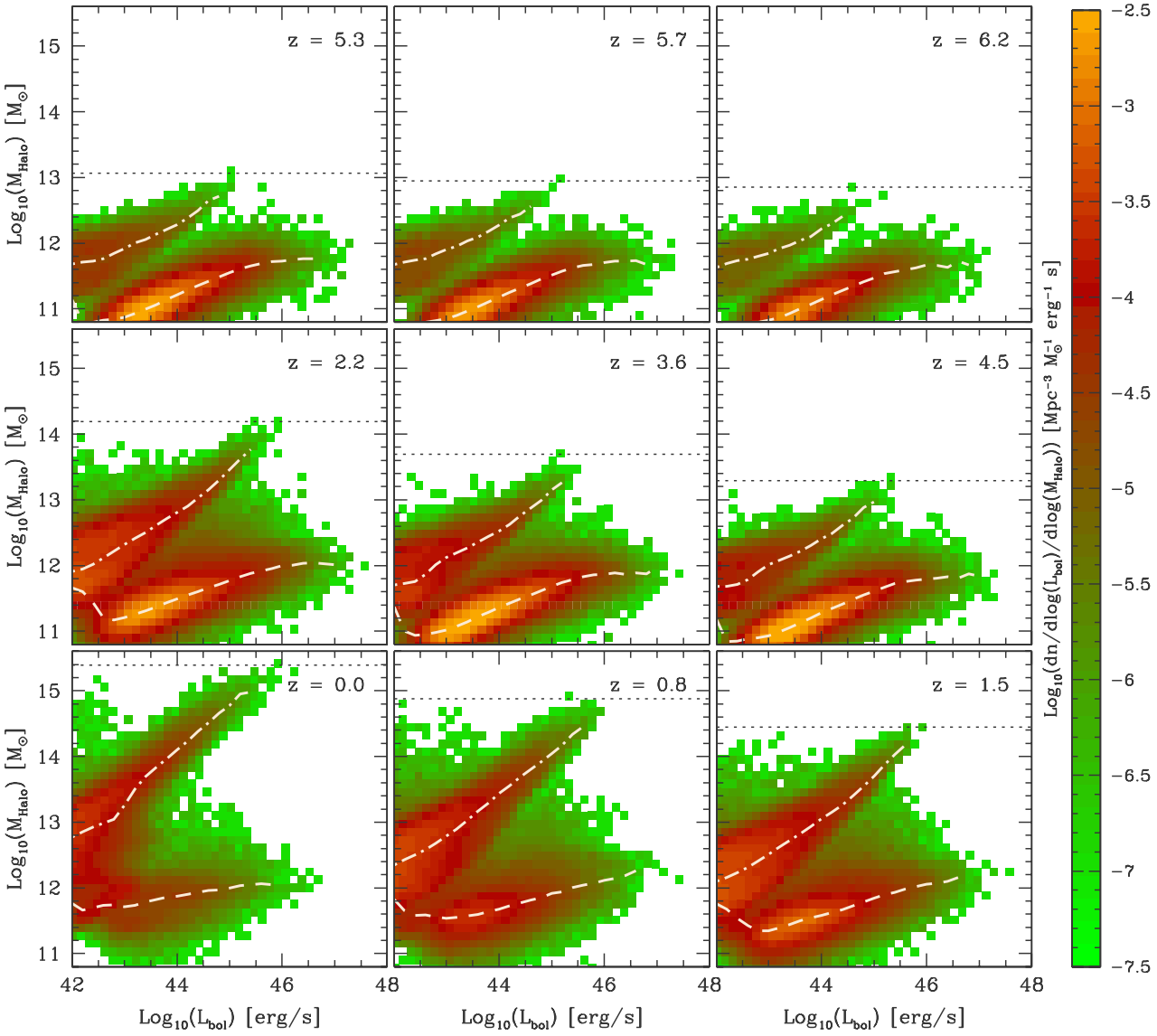

Figure 1. The correlation between bolometric luminosity and DM halo mass at $z = 0$-6.2 for the active galaxies in our model. Galaxies on the $L_{\rm bol}$-$M_{\rm Halo}$ plane are volume weighted as indicated by the colour bar. The horizontal dotted lines represent the mass of the most massive halo present in the simulation at that redshift. The white dashed and dash–dotted lines in each panel show the median of the $L_{\rm bol}$-$M_{\rm Halo}$ correlation for the starburst and hot-halo modes separately.

dependence of AGN. This is illustrated in Fig. 1, where we show how the bolometric luminosity correlates with the DM halo mass at $z = 0$-6.2. We also show the median of the $L_{\rm bol}$-$M_{\rm Halo}$ correlation in the starburst and hot-halo modes (dashed and dash–dotted lines, respectively) to help the reader distinguish the locus of each mode.

As illustrated by all redshift panels, AGN have a richly varied distribution on the $L_{\rm bol}$-$M_{\rm Halo}$ plane. Depending on the mode they accrete in, they are either found on the lower-middle part of the plane (starburst mode) or distributed diagonally upwards through the plane (hot-halo mode). In the starburst mode, the bulk of AGN is found in $\sim 10^{11}$–10^{12} $M_\odot$ haloes, although there is a very large scatter. In contrast, in the hot-halo mode we find a strong (positive) correlation between the halo mass and luminosity, which extends to halo masses of $\sim 10^{15}$ $M_\odot$. The shape of the two regimes remains the same with increasing redshift, but the relative density of AGN in the hot-halo mode changes significantly. At very high redshifts ($z \gtrsim 5$), the hot-halo branch almost vanishes, which is mainly due to the fact that not many DM haloes are subject to AGN feedback in the early universe (as we will describe in detail in the next sections). In contrast, the starburst mode becomes the dominant mode at high redshift, mostly due to the higher abundance of cold gas in galaxies in the early universe.

The typical stellar mass of AGN hosts also varies strongly. We show this in Fig. 2, where we now weight objects on the $L_{\rm bol}$-$M_{\rm Halo}$ plane according to their stellar mass, $M_{\rm star}$ (indicated by the colour bar on the right). As illustrated by the individual redshift bins, in the starburst mode we find a mild correlation of luminosity with stellar mass at $z < 1$, which spans approximately three orders of magnitude in stellar mass. We also find that the brightest objects, i.e. the QSOs, live in very massive systems with typical stellar masses of $M_{\rm star} \sim 10^{10}$–$10^{11}$ $M_\odot$. These objects are the remnants of massive disc galaxies that have recently experienced a disc instability, or occasionally a galaxy merger, and vast amounts of gas have become available for growing their central BH. Morphologically, these

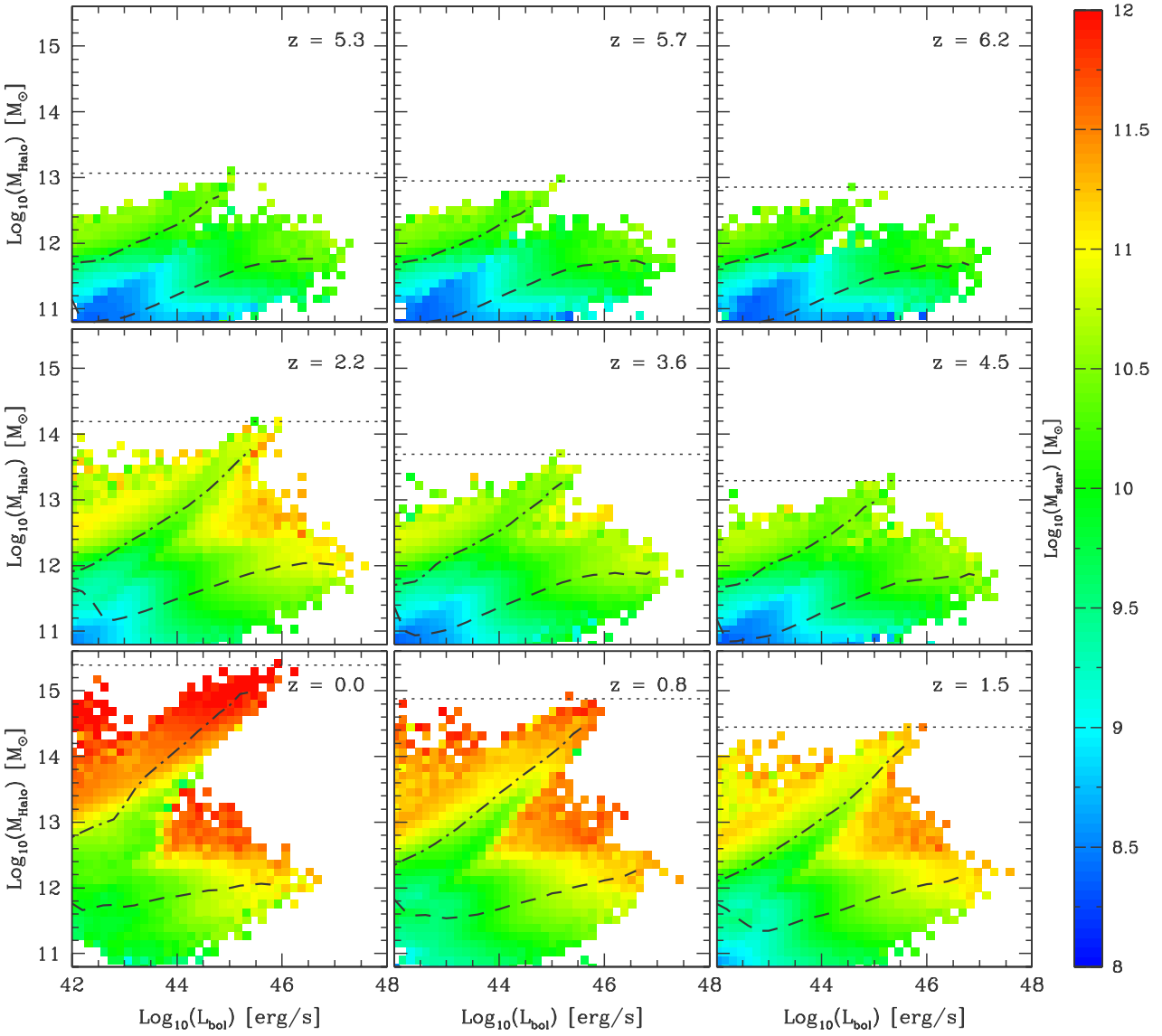

Figure 2. Same as in Fig. 1, with the colour shading now representing the median host stellar mass (in bins of $M_{\rm star}$), as indicated by the colour bar. The horizontal dotted lines represent the mass of the most massive halo at that redshift. The dashed and dash–dotted lines in every panel show the median of the $L_{\rm bol}$-$M_{\rm Halo}$ correlation for the starburst and hot-halo modes separately.

systems are spheroid dominated and tend to be oversized in stellar mass for their halo mass, as they represent the extreme scatter of the $M_{\rm Halo}$-$M_{\rm star}$ relation (Moster et al. 2010; Moster, Naab & White 2013). Given that they are characterized by high SF rates (triggered during the merger or disc instability), they *are not* associated with elliptical galaxies yet. The average halo mass of these luminous QSOs remains close to $\sim 10^{12}\,{\rm M}_{\odot}$ (with some considerable scatter), much lower than the typical halo masses of lower luminosity AGN.

For the AGN feedback to switch on in our model, it is necessary for the hot gas in the host halo to be in hydrostatic equilibrium. That is, the cooling time of the hot gas is much longer than a multiple of the free-fall time of the halo. In addition, the BH at the centre of the halo needs to be massive enough to efficiently heat the gas in the halo via the jet (see Bower et al. 2006 for the details of the AGN feedback mechanism). This typically occurs at a halo mass of 10^{12}–$10^{12.5}\,{\rm M}_{\odot}$ (the precise mass is controlled by a model parameter) and a BH mass of $10^{8.5}$–$10^{9}\,{\rm M}_{\odot}$. The most luminous QSOs satisfy these conditions. Therefore, it is expected that $M_{\rm star} \sim 10^{11}\,{\rm M}_{\odot}$ galaxies that undergo a significant QSO phase soon become subject to AGN feedback. Once this happens, the central BH accretes via the hot-halo mode, which is characterized by much lower accretion rates than the starburst mode. A fraction of the accretion luminosity produced during the hot-halo mode is coupled directly to the host halo and via the AGN feedback mechanism suppresses the cooling of hot gas.

The hosts of AGN in the hot-halo branch are usually very massive in stellar mass at $z \lesssim 1$. These AGN live in haloes where gas cooling and SF have been shut off by AGN feedback, and hence are red and dead. We associate these objects with the population of elliptical galaxies. Their central BHs accrete gas from the hot halo, and due to its low density, the bolometric luminosity of the accretion flow remains low (the geometry of the flow is usually that of an ADAF). Therefore, the majority of objects in this mode have a moderate-luminosity output, except from those in haloes of $\sim 10^{15}\,{\rm M}_{\odot}$ at low redshifts, where the central BH can shine as bright as $10^{46}\,{\rm erg\,s^{-1}}$

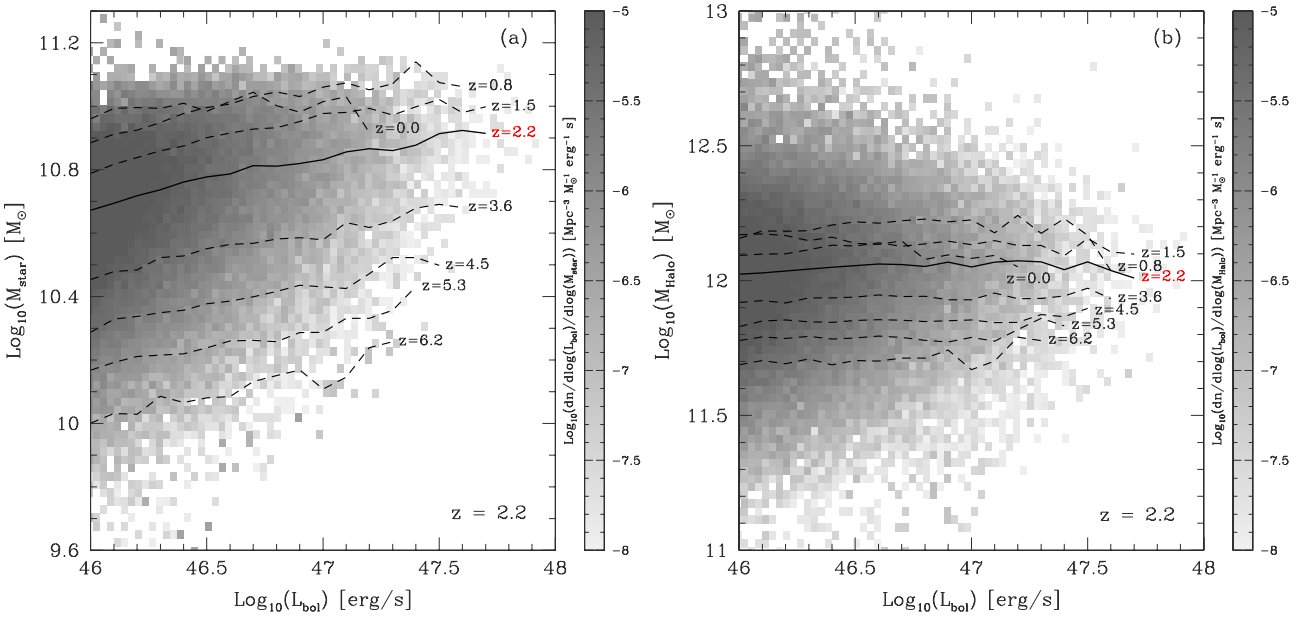

Figure 3. Left: the median of the $L_{\rm bol}$-$M_{\rm star}$ correlation for QSOs ($L_{\rm bol} \geq 10^{46}\,{\rm erg\,s^{-1}}$) and its evolution with redshift. The distribution of galaxies on the $L_{\rm bol}$-$M_{\rm star}$ plane is shown at $z = 2.2$ (in a similar fashion as in Fig. 1) as an indication of the extent of the scatter around the median. Right: similar to the left-hand panel, but for the $L_{\rm bol}$-$M_{\rm Halo}$ correlation.

(these objects have relatively high accretion rates and thus form a radiatively efficient thin disc).

To obtain a better understanding of the typical hosts of QSOs, we show in Fig. 3 how the median stellar mass of QSOs varies with the luminosity and redshift. In the same figure, we also plot the distribution of galaxies on the $L_{\rm bol}$-$M_{\rm Halo}$ plane at $z = 2.2$ to show the typical extension of the scatter around the median. As illustrated by the plot, the hosts of QSOs tend to become more massive with time. In fact, the host galaxies of QSOs of a given luminosity are approximately one order of magnitude more massive than the hosts of QSOs of the same luminosity at $z \sim 6$. This primarily relates to the fact that the cold-gas reservoir in galaxies becomes increasingly smaller as redshift decreases. At fixed redshift, we find that the host stellar mass of QSOs shows a mild dependence on bolometric luminosity, which translates into an increase of approximately 0.4 dex in stellar mass between 10^{46} and $10^{48}\,{\rm erg\,s^{-1}}$. The mild dependence is due to the fact that the accretion time-scale increases with stellar mass in the host bulge. Therefore, an increase in stellar mass (that in principle implies an increase of the cold gas available for feeding the BH) causes a similar increase in the accretion time-scale, which then results in a weak luminosity dependence.

In contrast to the stellar mass, the DM halo mass of QSOs shows no dependence on luminosity. This is shown in Fig. 3(b), where we plot the median of the $M_{\rm Halo}$-$L_{\rm bol}$ correlation of QSOs in a similar fashion as in Fig. 3(a). Therefore, at a given redshift, QSO activity usually takes place in the same type of DM environment, which is independent of luminosity. At $z \lesssim 2$, this environment is similar to a typical Milky Way halo.

Finally, from Fig. 1 we see that at $z \lesssim 1.5$ the number density of objects accreting in the hot-halo mode is relatively high. Therefore, we expect these objects to influence strongly the typical environment of the 10^{44}–$10^{46}\,{\rm erg\,s^{-1}}$ AGN. We explore this topic in Fanidakis et al. (2013), where we show that our prediction for the typical DM halo mass of moderate-luminosity AGN is much higher than that of luminous QSOs. This is in excellent agreement with clustering studies of moderate-luminosity X-ray selected AGN (Coil et al. 2009; Gilli et al. 2009; Cappelluti et al. 2010; Krumpe, Miyaji & Coil 2010; Allevato et al. 2011; Starikova et al. 2011; Krumpe et al. 2012; Mountrichas & Georgakakis 2012, see also Koutoulidis et al. 2013).

3.2 The effective halo mass of QSOs

The clustering of QSOs depends both on the clustering of DM haloes and on how QSOs occupy these haloes. On large scales, the QSOs have a constant clustering bias $b_{\rm eff}$ given by (Baugh et al. 1999)

$$b_{\rm eff}(z) = \frac{\int b(M_{\rm Halo}, z) N_{\rm q}(M_{\rm Halo}, z) n(M_{\rm Halo}, z)\, {\rm d}\log M_{\rm Halo}}{\int N_{\rm q}(M_{\rm Halo}, z) n(M_{\rm Halo}, z)\, {\rm d}\log M_{\rm Halo}}, \qquad (4)$$

where $b(M_{\rm Halo}, z)$ is the linear clustering bias of haloes of mass $M_{\rm Halo}$, $N_{\rm q}(M_{\rm Halo}, z)$ is the mean number of QSOs in a halo of mass $M_{\rm Halo}$ and $n(M_{\rm Halo}, z)\,{\rm d}\log M_{\rm Halo}$ is the number density of haloes in the logarithmic interval ${\rm d}\log M_{\rm Halo}$. The clustering of QSOs can be measured from observational surveys and the value of $b_{\rm eff}$ inferred. The effective halo mass $M_{\rm Halo,\,eff}$ for the QSO sample is then calculated from the measured $b_{\rm eff}$ by inverting the halo bias relation, using $b_{\rm eff} = b(M_{\rm Halo,\,eff}, z)$. We calculate $M_{\rm Halo,\,eff}$ from $b_{\rm eff}$ using the ellipsoidal collapse model of Sheth & Tormen (1999). Therefore, the model predictions can be compared directly to the observational estimation of QSO halo masses from clustering surveys such as SDSS and 2dF.

The $M_{\rm Halo,\,eff}$ of QSOs as a function of redshift is shown in Fig. 4 (solid red line). As illustrated by the plot, $M_{\rm Halo,\,eff}$ remains close to $\sim 10^{12.4}\,{\rm M_\odot}$ for QSOs in the low-redshift universe, and drops by $\sim$0.2 dex as z increases. Such a halo mass is representative of a typical Milky Way halo environment. This prediction is consistent with what clustering analyses of QSOs in galaxy surveys indicate (Croom et al. 2005; Ross et al. 2009), namely that QSOs in the low-z Universe tend to live in average DM environments. We note that, to produce such high luminosities as $10^{48}\,{\rm erg\,s^{-1}}$, a vast amount of gas is required to be accreted, which is why we find our brightest

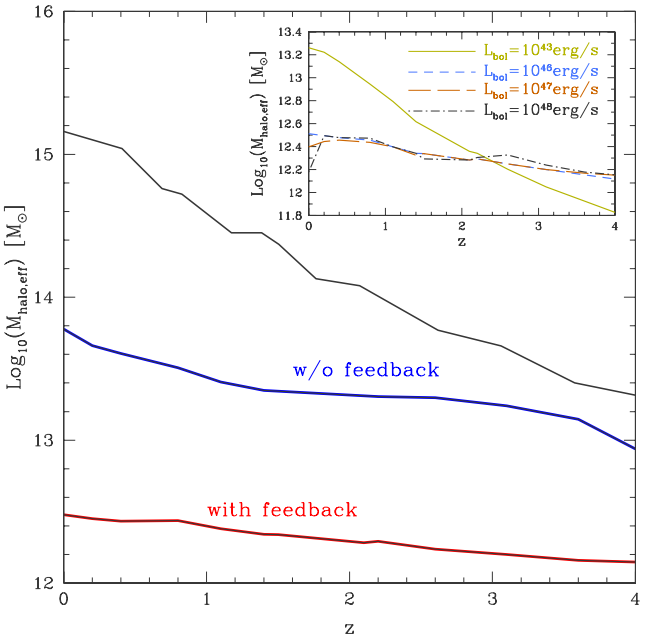

Figure 4. The effective DM halo mass of QSOs ($L_{\rm bol} \geq 10^{46}\,{\rm erg\,s^{-1}}$) as a function of redshift (solid red line). Predictions are also shown for a simulation where AGN feedback is not taken into account (blue solid line). The grey solid line represents the mass of the most massive halo in the simulation at a given redshift. Inset panel: effective DM halo mass as a function of redshift for four different luminosity AGN populations, as indicated by the key (QSOs are represented by the $L_{\rm bol} = 10^{46}$, 10^{47} and $10^{48}\,{\rm erg\,s^{-1}}$ populations).

sources in the most gas rich (and massive) galaxies (see Fig. 3a). Yet, from Fig. 3(b) we expect that even these extreme objects should be found in haloes of similar mass ($\sim 10^{12}\,{\rm M_\odot}$) to the hosts of average luminosity QSOs. We show this in the inset panel of Fig. 4, where we plot $M_{\rm Halo,\,eff}$ as a function of redshift for different luminosity AGN populations ($L_{\rm bol} = 10^{43}$, 10^{46}, 10^{47} and $10^{48}\,{\rm erg\,s^{-1}}$). The expected environment of QSOs ($L_{\rm bol} \geq 10^{46}\,{\rm erg\,s^{-1}}$) is the same for all luminosity populations, with only insignificant variations at low redshift. In contrast, AGN belonging to much less luminous classes (e.g., $L_{\rm bol} = 10^{43}\,{\rm erg\,s^{-1}}$) tend to live in haloes more massive by an order of magnitude at low redshift.

Finally, in Fanidakis et al. (2013), we suggest that the luminosity output of an AGN is determined by the accretion channel and ultimately by the DM halo mass of the AGN host. For example, haloes that are subject to AGN feedback can only host AGN whose accretion flow is relatively underdense and therefore produce moderate luminosities (10^{44}–$10^{46}\,{\rm erg\,s^{-1}}$). Accretion in this case is fed directly by the hot halo around the galaxy. In this picture, QSOs can only exist in average environments where AGN feedback is not present, and thus, gas in the host halo can cool efficiently. The importance of AGN feedback in defining the halo mass of bright QSO is illustrated by the blue line in the main panel of Fig. 4, which shows $M_{\rm Halo,\,eff}$ for QSOs in a simulation where AGN feedback is turned off. In this case, the typical halo mass of QSOs[2] increases dramatically, making their environment that of the very massive haloes. In fact, the largest halo at a given redshift (indicated by the solid grey line in the plot) is now found to host a very bright QSO with typical luminosity of $\sim 10^{47}$–$10^{48}\,{\rm erg\,s^{-1}}$. Hence, in a universe without AGN feedback, galaxy groups and clusters should be the typical environments where enormous QSO activity takes place. However, in our observable Universe, bright QSOs are never observed in the cores of clusters in the low-redshift Universe.

[2] In this simulation, we consider all AGN with $L_{\rm bol} \geq 10^{46}\,{\rm erg\,s^{-1}}$ as QSOs. We note that, in this case, the model has not been tuned to fit the observational data. Requirement of retuning the accretion model might result in lower AGN luminosities, however, without affecting the clustering of these sources much.

4 THE ENVIRONMENT OF FIRST QSOS

As mentioned earlier, $z \sim 6$ QSOs are of particular interest, since they are assumed to reside in overdensities and pinpoint the location of protoclusters. Here we test this idea by considering the $z \sim 6$ QSOs in our model and exploring the properties of their DM halo environment and their descendants at $z = 0$. We also provide a calculation for the number of LBGs expected to be found around $z \sim 5$ QSOs in order to provide a better understanding of the observations that search for galaxy overdensities around high-z QSOs.

4.1 The $z = 6.2$ QSOs and their descendants to $z = 0$

In this section, we explore the environment of high-z QSOs and present predictions for their descendants at $z = 0$. We do so by showing in Fig. 5 how QSOs (filled circles) populate the $L_{\rm bol}$-$M_{\rm Halo}$ plane at $z = 6.2$. In the same plot, we also show all DM haloes (filled squares) with $M_{\rm Halo} > 10^{12}\,{\rm M_\odot}$ that host an AGN. We sample these objects from a subvolume of $200\,h^{-1}$ Mpc of the simulation to avoid overfilling the plot (yet the volume is large enough to exclude cosmic variance effects). Objects on the $L_{\rm bol}$-$M_{\rm Halo}$ plane are colour coded according to their descendant halo mass at $z = 0$, as indicated by the

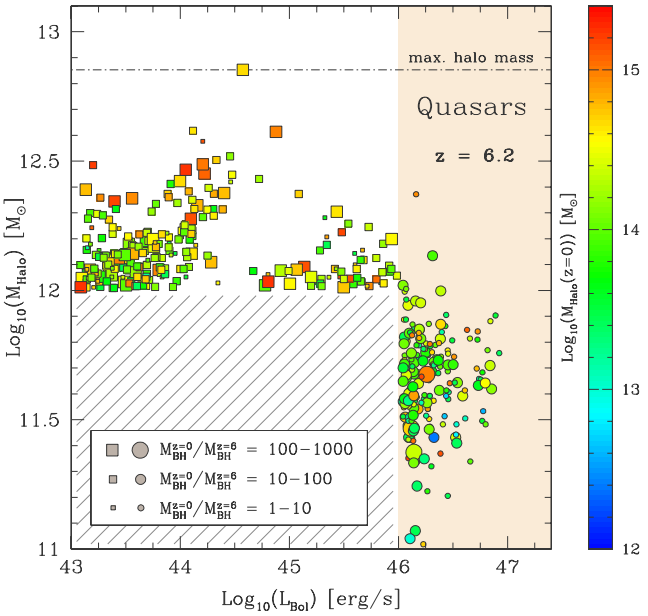

Figure 5. Bolometric luminosities and DM halo masses for $z = 6.2$ QSOs (filled circles). We also plot all haloes with masses greater than $10^{12}\,{\rm M_\odot}$ that host an AGN (filled squares). The symbols are colour coded according to the halo mass of the $z = 0$ descendant, as indicated by the colour bar on the right. The symbol sizes indicate the ratio of the QSO descendant BH mass at $z = 0$ over its BH mass at $z = 6.2$. The dash–dotted horizontal line indicates the mass of the most massive halo at $z = 6.2$. The hatched area represents the part of the plane that is not sampled for clarity reasons.

colour bar on the right. In addition, the size of the symbols indicates the ratio of the central BH mass at $z = 0$ to that at $z = 6.2$

According to Fig. 5, our model suggests that the halo hosts of luminous QSOs at $z = 6.2$ span an order of magnitude in mass, which always remains between $\sim 10^{11}$ and $10^{12}\,\mathrm{M}_\odot$ (with only one or two exceptions higher than $10^{12}\,\mathrm{M}_\odot$). When considering the extremes of the QSO population, we find that the brightest QSO at $z = 6.2$ has a bolometric luminosity of $10^{46.9}\,\mathrm{erg\,s^{-1}}$ and a host halo mass of $\sim 10^{11.8}\,\mathrm{M}_\odot$. Its descendant at $z = 0$ is a central elliptical galaxy with stellar mass of $\sim 10^{11.4}\,\mathrm{M}_\odot$ in a DM halo of mass $10^{13.4}\,\mathrm{M}_\odot$. Interestingly, the BH harboured by this QSO has grown by a factor of 6 in mass by $z = 0$.

The galaxy descendants of the rest of the $z = 6.2$ QSOs show a wide range of morphologies. A great fraction of them (25 per cent) evolve into pure spheroids ($B/T = 1$), but we also find a non-zero fraction (3 per cent) of disc galaxies ($B/T \leq 0.5$). These can be central or satellite galaxies in a variety of haloes (frequently also in $10^{14}\,\mathrm{M}_\odot$ haloes) with relatively low stellar masses ($\sim 5 \times 10^{10}\,\mathrm{M}_\odot$). The characteristics of pure spheroidal descendants (which at $z = 0$ are elliptical galaxies) are also quite diverse, although they do tend to be massive ($\gtrsim 10^{11}\,\mathrm{M}_\odot$) and centrals. In these galaxies, we find that BHs usually grow more efficiently and, as seen in Fig. 5, in some of the descendants the central BH has grown by more than two to three orders of magnitude in mass since $z \sim 6$. Interestingly, we find no apparent correlation between $z = 6.2$ QSO luminosity and descendant halo mass, stellar mass or morphology.

Similarly to the low-z universe, the most massive haloes tend to avoid hosting a QSO. This result is in contrast with what is usually assumed, as outlined previously. A great fraction of haloes at $z = 6.2$ with masses higher than $10^{12}\,\mathrm{M}_\odot$ are found to host an AGN of moderate luminosity. The most massive halo at $z = 6.2$ ($M_{\rm Halo} = 10^{12.85}\,\mathrm{M}_\odot$) does host an AGN, its luminosity though is relatively low and equal to $\sim 10^{44.6}\,\mathrm{erg\,s^{-1}}$, which makes it too faint to be detected with current instruments. The halo descendant of the most massive halo at $z = 6$ has a mass of $10^{14.7}\,\mathrm{M}_\odot$ and hosts a massive elliptical with $M_{\rm star} = 10^{11.5}\,\mathrm{M}_\odot$. Interestingly, this is not the most massive DM halo in our cosmological volume at $z = 0$. This is in agreement with recent findings by Angulo et al. (2012). These authors showed that in a hierarchical universe, the future growth of a $z \sim 6$ DM halo is more determined by the environment on scales of ~ 10 Mpc than by the actual halo mass, as the former is expected to be the main factor shaping the future halo mass assembly (see also De Lucia & Blaizot 2007; Trenti et al. 2008; Overzier et al. 2009).

The lack of QSOs in the most massive DM haloes in the early universe is due to the universality of the AGN feedback mechanism. Even at such high redshifts, haloes with masses greater than $\sim 10^{12}\,\mathrm{M}_\odot$ become subject to feedback. Their space density is very low ($<10^{-8}\,\mathrm{Mpc^{-3}}$), nevertheless, as we shall show in a forthcoming study, BH growth and QSO activity in these environments are considerably affected by AGN feedback. Similar conclusions have been reached by Di Matteo et al. (2012, see also DeGraf et al. 2012). These authors have employed high-resolution smoothed particle hydrodynamic simulations of the growth of BHs in the early universe (with a box size of $0.75\,h^{-1}$ Gpc) to show that the most massive haloes ($M_{\rm Halo} \gtrsim 10^{12}\,\mathrm{M}_\odot$) by $z = 6$ have already shut off SF and QSO activity at their centres due to feedback. However, our model contradicts the predictions of Springel et al. (2005). In their work, Springel et al. assume that the first QSOs are associated with the galaxies that have the highest SF rates. Using a semi-analytical model (Croton et al. 2006), they show that galaxies with the highest SF rates identify with objects with the highest stellar and virial mass. Thus, the first QSOs are always expected to be harboured by the most massive DM haloes. In our model, galaxies with high SF rates live in the same environment as the most luminous QSOs and therefore not in the most massive haloes. Our predictions differ from those of Springel et al. (2005) because the AGN feedback mechanism is much more efficient in quenching the cooling of gas at high redshift than in their model. A very efficient feedback mechanism in our model is necessary for reproducing observations of galaxies and AGN in a wide redshift range ($0 < z < 6$).

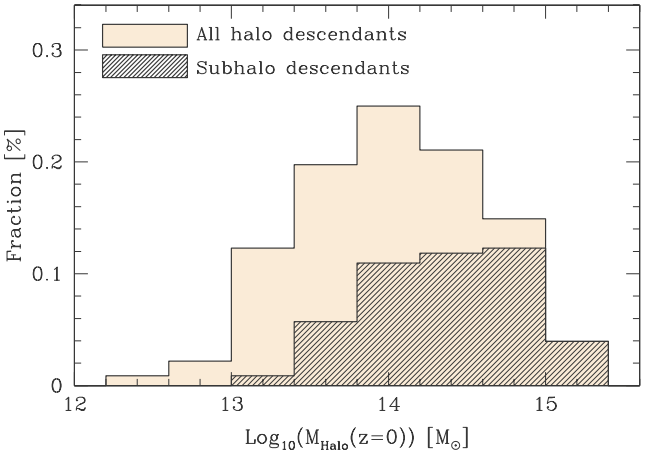

Figure 6. The halo mass distribution at $z = 0$ of the descendants of $z = 6.2$ QSOs. The filled histogram shows the fraction of QSO descendants that evolve into haloes of mass $\log M_{\rm Halo}$ at $z = 0$. The hatched histogram shows those QSO descendants that are identified as substructures (satellite subhaloes) in DM haloes of mass $\log M_{\rm Halo}$ at $z = 0$.

The $z = 0$ halo descendants of luminous QSOs are characterized by a wide range of masses (typically higher than $10^{13}\,\mathrm{M}_\odot$). This is shown in Fig. 6, where we plot the $z = 0$ halo mass distribution of the descendants of $z = 6.2$ QSOs. The majority of them are found in rich clusters with a mass of $\sim 10^{14}\,\mathrm{M}_\odot$. Trenti et al. (2008) have reached a similar conclusion by means of the extended Press–Schechter formalism (even though they assume that the brightest QSOs at $z \sim 6$ live in the most massive DM haloes). This again confirms the picture that the most massive haloes formed at high redshift usually evolve into more typical structures at $z = 0$. We also find that in the present-day universe, 46 per cent of the descendants are located in DM haloes with mass in the range 10^{13}–$10^{14}\,\mathrm{M}_\odot$, a similar percentage in haloes with mass of 10^{14}–$10^{15}\,\mathrm{M}_\odot$ and only 4.2 per cent in haloes more massive than $10^{15}\,\mathrm{M}_\odot$. Thus, high-$z$ QSOs are more likely to trace the progenitors of rich clusters ($M_{\rm Halo} \sim 10^{14}\,\mathrm{M}_\odot$) than superclusters ($M_{\rm Halo} \sim 10^{15}\,\mathrm{M}_\odot$). Furthermore, many of these descendants are identified only as satellite subhaloes at $z = 0$. For example, in the mass regime of 10^{14}–$10^{15}\,\mathrm{M}_\odot$, we find that 62 per cent of the descendants are satellite subhaloes. In haloes more massive than that ($M_{\rm Halo} \geq 10^{15}\,\mathrm{M}_\odot$), the fraction reaches 100 per cent, and therefore, QSO descendants in the most massive haloes at $z = 0$ are identified only as satellites. As a final note, we find that the QSO hosts that evolve to $z = 0$ haloes with mass $\geq 10^{14}\,\mathrm{M}_\odot$ represent a fraction of only 0.02 per cent of the total halo population at $z = 0$ with such mass. Therefore, only a negligible fraction of the today's most massive haloes had progenitors which hosted a QSO at $z = 6.2$, which implies that the probability that a massive DM structure today harboured a $z \sim 6$ QSO is almost zero.

The properties of QSOs on the $L_{\rm bol}$-$M_{\rm Halo}$ plane in Fig. 5 are confirmed also when we consider how QSOs are distributed in the

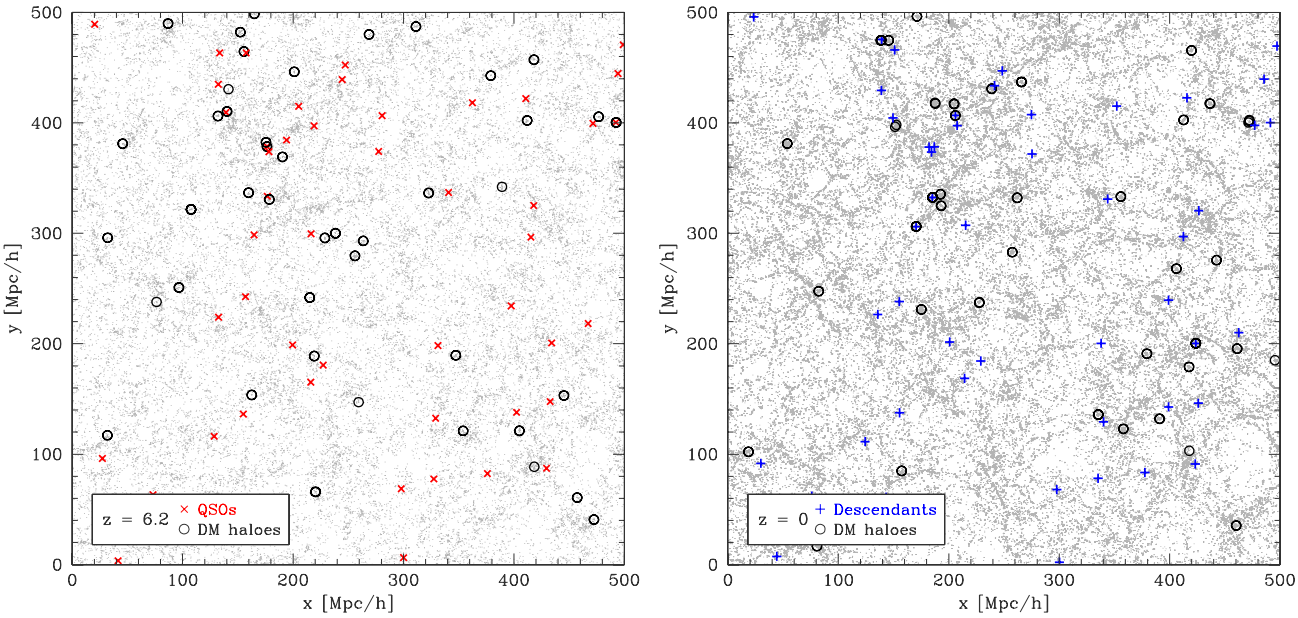

Figure 7. Spatial maps of QSOs and the most massive DM haloes. Left: the spatial distribution of QSOs (red crosses) and the most massive DM haloes (black circles) at $z = 6.2$ in our simulation. Right: the spatial distribution of the descendant DM haloes of $z = 6.2$ QSOs (blue crosses) and the most massive haloes ($M_{\rm Halo} \geq 10^{12}\,{\rm M}_{\odot}$) at $z = 0$. The thickness of each slice is $100\,h^{-1}$ Mpc along the z direction. In both panels, the number of DM haloes depicted equals the number of QSOs. The underlying DM distribution is shown in grey. At both redshifts, there is a mismatch in the positions of the brightest QSOs (or the descendants) and the most massive haloes that are in place.

cosmic web. We show this in Fig. 7, where we plot the spatial distribution of QSOs relative to that of the most massive DM haloes at $z = 6.2$ (left-hand panel) and the distribution of their descendants at $z = 0$ (right-hand panel). At $z = 6.2$ we find that in the majority of the cases QSOs avoid the environments of the extreme DM peaks. In the cases where the position of QSOs coincides with that of the largest DM haloes, we find that the host halo has a mass of $\sim 10^{12}\,{\rm M}_{\odot}$, in accordance with Fig. 5. At $z = 0$, we find that the QSO descendants are found in less extreme environments of the DM distribution, yet occasionally also in the most massive haloes. This picture illustrates again that some of the most massive DM haloes at $z = 0$ could have hosted a bright QSO at $z = 6.2$. However, detecting a bright QSO at $z = 6.2$ does not guarantee that its host halo is a progenitor of a massive halo at $z = 0$.

4.2 Overdensities around $z \sim 5$ QSOs

As we saw previously, the halo mass of low-z QSOs is well below the mass of the most massive structures of the DM distribution. For the majority of QSOs, their environment is representative of that of the average mass DM haloes. However, at $z \sim 6$ the mass of the most massive haloes is only an order of magnitude higher than the typical halo mass of QSOs. Therefore, we should expect an enhancement of structures near these QSOs (especially for those hosted by $10^{12}\,{\rm M}_{\odot}$ haloes), yet not as strong as the overdensities in the most massive haloes.

Husband et al. (2013) recently presented an observational study of the clustering of LBGs in three QSO fields at $z \sim 5$. These authors employed spectroscopically identified LBGs in the European Southern Observatory Remote Survey (ERGS; Douglas et al 2009, 2010) and showed that two of the three fields show an overdensity of galaxies within a narrow redshift range of $\Delta z = 0.05$. When comparing to the clustered structures identified in the ERGS, the authors conclude that QSO environments are overdense, yet not more extreme than rich structures in the field. Here, we test this observation by calculating the number of LBGs expected to be found near a QSO in our simulation.

We model LBGs as in Lacey et al. (2011), by taking into account the attenuation of starlight by the dust content of the galaxy. The predictions of the model for the abundance of LBGs match the observed LBG LF over a wide range of redshifts ($3 < z < 10$; see Lacey et al., in preparation). Our sample of LBGs considers all galaxies with far-UV (1500 Å) luminosities in the range of the observed LBG LF at $z \sim 5$, i.e. $M_{\rm AB}(1500\,{\rm \AA}) \leq -16$. With this luminosity cut, the model predicts an LBG space density of $1.3 \times 10^{-3}\,{\rm Mpc}^{-3}$. We determine the number of expected LBG neighbours by counting the total number of LBGs within a sphere of comoving radius 10 Mpc centred around the QSO and normalize it in units of the mean. The integration radius of 10 Mpc is half the comoving distance that corresponds to a separation of $\Delta z = 0.05$ at $z = 4.9$ and we choose this value in order to be consistent with the Husband et al. observations. Our predictions at $z = 4.9$ for the quantity $\delta_{\rm LBG}(r) = N_{\rm LBG}(r)/\langle N_{\rm LBG}(r)\rangle$ are shown in Fig. 8. We also show the expected number of LBGs in the field and in the most massive (extreme) DM structures by selecting all DM haloes with $10^{11} < M_{\rm Halo} < 5 \times 10^{12}\,{\rm M}_{\odot}$ and $M_{\rm Halo} \geq 5 \times 10^{12}\,{\rm M}_{\odot}$, respectively. We do not consider haloes less massive than $10^{11}\,{\rm M}_{\odot}$ in the calculation of the field abundance due to the low resolution of the simulation below that mass.

According to Fig. 8(a), our model suggests that the overdensities of LBGs expected to be found within 10 Mpc from a QSO are similar to that found in the field. QSO fields that show an excess of sources are typically two to three times more dense than the average density of LBGs in the universe. We also find QSOs that show much higher enhancements but their frequency is very low. Interestingly, given that the there is a difference in the overdensity distributions of field and QSO haloes at $\delta > 1$, we expect that an overdensity is slightly more likely to be found around a QSO than in the field. This is in good agreement with the analysis of Husband et al. On the other

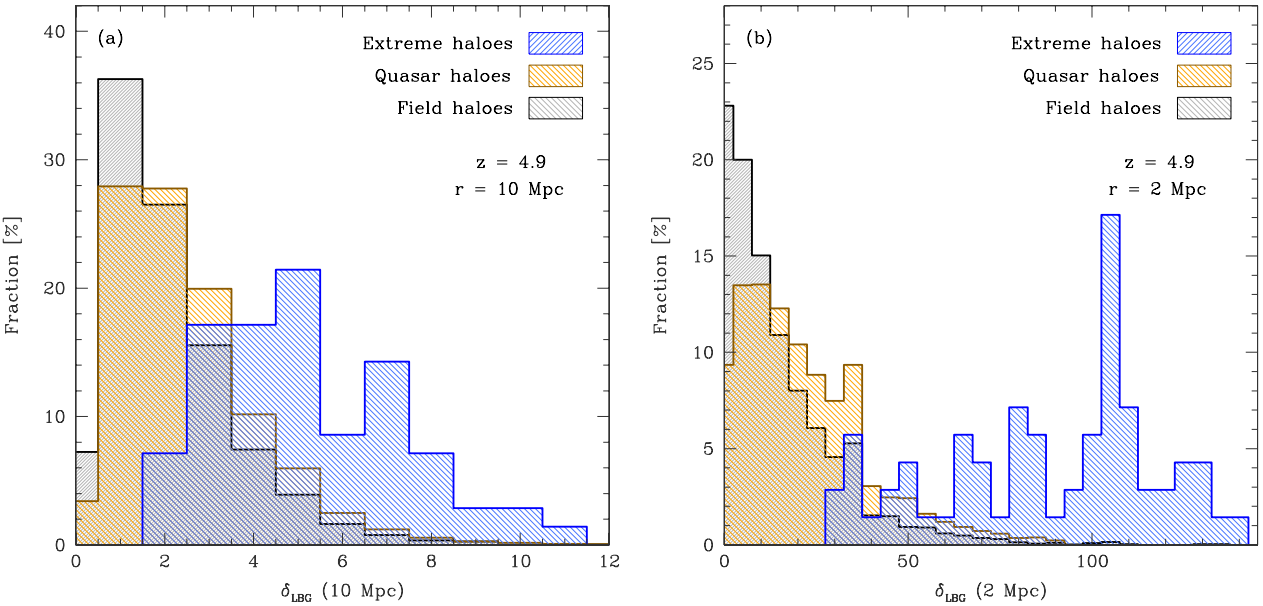

Figure 8. Left: the fraction of DM haloes at $z = 4.9$ characterized by an overdensity $\delta_{\rm LBG}(r)$ of LBGs on a scale of $10\,h^{-1}$ Mpc. $\delta_{\rm LBG}(r)$ is defined as $N_{\rm LBG}(r)/\langle N_{\rm LBG}(r)\rangle$. The different histograms represent the haloes that host QSOs (orange shading), the most massive DM haloes ($M_{\rm Halo} \geq 5 \times 10^{12}\,{\rm M}_{\odot}$, blue shading) and the 'field' DM haloes ($10^{11} < M_{\rm Halo} < 5 \times 10^{12}\,{\rm M}_{\odot}$, grey shading). The lower luminosity cut for the LBG sample is $M_{\rm AB}(1500\,{\rm \AA}) = -16$. Right: same as the left-hand panel but for $\delta_{\rm LBG}(r)$ calculated at $2\,h^{-1}$ Mpc.

hand, LBGs cluster strongly near the most massive haloes, where we find that the typical overdensity has an abundance of LBGs five to seven times higher than the average value. Therefore, we expect a considerable number of LBGs at the extremes of the DM distribution, usually higher than the number found around QSOs. Thus, although an enhancement of galaxies is expected to be found around $z \geq 5$ QSOs (with a frequency higher than when searching blank fields), it is likely that it will be considerably lower than that expected in the most massive structures.

The comoving separation of the detected LBGs in the Husband et al. sample could be large enough to select galaxies which may not be physically related to the QSO. The redshift separation $\Delta z = 0.05$ is indeed quite narrow compared to previous studies, yet it still corresponds to a region of 20 Mpc in size. On such big scales when we count neighbours around a QSO in our simulation, we might be selecting galaxies that belong to an actual overdensity (i.e. of an extreme halo), but not to the QSO itself. We find that an ideal integration radius for selecting only galaxies that are physically related to the QSO is approximately 2 Mpc. This is a representative radius of a collapsing region at $z \sim 6$. In Fig. 8(b), we show how the predictions in Fig. 8(a) change when we consider an integration radius of 2 Mpc. The general picture described in the previous paragraph does not change. However, now we find a more clear separation between the QSO and extreme halo distributions. This implies that in an ideal survey of LBGs with a very narrow redshift separation, the most massive haloes at that redshift should show very distinct, and extreme, overdensities. An integration field of length of 4 Mpc at $z \sim 5$ corresponds to a redshift separation of $\Delta z = 0.01$. Thus, forthcoming observational studies need to detect objects within this redshift separation in order to clearly separate QSO fields from the most extreme overdensities in the Universe.

We note that our predictions are very sensitive to the luminosity cut of the LBG sample. Surveys that do not reach magnitudes as faint as the ones we consider here will of course detect a lower number of objects. When considering brighter samples we find an overall decrease in the number of LBGs around QSOs, field and extreme haloes, yet the overall picture does not change much. Hence we conclude that, although it is very likely to find an overdensity of galaxies around a QSO compared to the field, the actual extremes of the DM distribution show a much stronger clustering signal compared to the environments traced by QSOs.

5 SUMMARY AND CONCLUSIONS

We have presented an analysis of the DM halo environment of QSOs (active galaxies with bolometric luminosities greater than $10^{46}\,{\rm erg\,s^{-1}}$) using the semi-analytic model GALFORM. In this model, BHs grow via two accretion channels related to episodes of galaxy mergers and disc instabilities in the host galaxy (starburst mode) and direct accretion from the hot halo around the galaxy in massive haloes ($M_{\rm Halo} \gtrsim 10^{12.5}\,{\rm M}_{\odot}$; hot-halo mode). A key ingredient of this model is the AGN feedback mechanism which operates in $\gtrsim 10^{12.5}\,{\rm M}_{\odot}$ haloes and shuts off cooling in the halo and SF in the central galaxy. The feedback mechanism is directly linked to the hot-halo mode accretion channel, as it is assumed that gas accretion in this mode enables a thermal coupling of the central BH engine to the gas in the host DM halo.

By means of this model, we have shown that QSOs live in average environments with a typical halo mass of $\sim 10^{12}\,{\rm M}_{\odot}$. This halo mass remains approximately constant up to $z \sim 4$ and is insignificantly dependent on luminosity. The triggering of QSO activity in higher mass haloes is usually inhibited by the AGN feedback mechanism. When switching off feedback in our calculation, we find a typical halo mass higher than $10^{13}\,{\rm M}_{\odot}$. This is in contrast with the observational estimates from SDSS and 2dF. Therefore, AGN feedback is necessary not only for reproducing the right shape of the galaxy LF, but also the halo environment of QSOs.

At higher redshifts, QSOs reside in massive haloes that have not yet become subject to feedback. At $z \sim 6$ these haloes have masses of 10^{11}–$10^{12}\,{\rm M}_{\odot}$, almost an order of magnitude lower than

the mass of the most massive bound structures at that redshift. The $z = 0$ descendants of these haloes span a wide range of halo masses, stellar content and DM halo masses. QSOs typically evolve into spheroidal galaxies (which are associated with elliptical galaxies), typically found in rich clusters ($M_{\rm Halo} \sim 10^{14}\,{\rm M}_{\odot}$). We also find that a non-zero fraction (3 per cent) of these QSOs have evolved into disc satellites in massive haloes ($M_{\rm Halo} = 10^{13}$–$10^{14}\,{\rm M}_{\odot}$), with their central BHs having grown only by a factor of a few since $z \sim 6$. When we consider the halo descendants of $z \sim 6$ QSOs, we find that the majority of them are located in haloes with masses of $\sim 10^{14}\,{\rm M}_{\odot}$. A negligible fraction of descendants are located in haloes of $10^{15}\,{\rm M}_{\odot}$ and they are always identified as satellite subhaloes. Due to the low fraction of descendants in the most massive haloes at $z = 0$, we conclude that $z \sim 6$ QSOs as cosmological probes are more likely to trace the progenitors of present-day rich clusters ($M_{\rm Halo} \sim 10^{14}\,{\rm M}_{\odot}$).

Regarding the abundance of galaxies detected around high-z QSOs, we find that when searching the fields of $z \sim 5$ QSOs, it is very likely to find an overdensity of galaxies. In fact, the probability of finding one is higher than when searching blank fields. However, the overdensities usually detected around QSOs are not as extreme as those expected in the most massive haloes at that redshift. Therefore, observations that find overdensities around QSOs do not really probe the peaks of the DM distribution. The model also predicts a significant number of QSOs that do not reside in an overdensity. The same picture seems to hold also at $z \sim 6$.

To conclude, we have shown that the halo mass of QSOs at all redshifts does not coincide with that of the most massive structures of the DM distribution. This study is a first step towards understanding the environment of QSOs in the low- and high-z universe. In a forthcoming paper, we will explore in detail the complete evolution through cosmic time of the first QSOs in order to understand better the nature of the most luminous objects in the Universe.

ACKNOWLEDGEMENTS

The authors would like to thank Raul Angulo and Aaron Dutton for valuable comments. AVM acknowledges financial support to the DAGAL network from the People Programme (Marie Curie Actions) of the European Union's Seventh Framework Programme FP7/2007- 2013/ under REA grant agreement number PITN-GA-2011-289313. CMB acknowledges Max-Planck-Institut für Astronomie for its hospitality and financial support through the Sonderforschungsbereich SFB 881 'The Milky Way System' (subproject A1) of the German Research Foundation (DFG).

REFERENCES

Allevato V. et al., 2011, ApJ, 736, 99
Angulo R. E., Springel V., White S. D. M., Cole S., Jenkins A., Baugh C. M., Frenk C. S., 2012, MNRAS, 425, 2722
Bañados E., Venemans B., Walter F., Kurk J., Overzier R., Ouchi M., 2013, ApJ, 773, 178
Bardeen J. M., Bond J. R., Kaiser N., Szalay A. S., 1986, ApJ, 304, 15
Baugh C. M., 2006, Rep. Prog. Phys., 69, 3101
Baugh C. M., Benson A. J., Cole S., Frenk C. S., Lacey C. G., 1999, MNRAS, 305, L21
Baugh C. M., Lacey C. G., Frenk C. S., Granato G. L., Silva L., Bressan A., Benson A. J., Cole S., 2005, MNRAS, 356, 1191
Benson A. J., 2010, Phys. Rep., 495, 33
Bonoli S., Marulli F., Springel V., White S. D. M., Branchini E., Moscardini L., 2009, MNRAS, 396, 423
Bonoli S., Shankar F., White S. D. M., Springel V., Wyithe J. S. B., 2010, MNRAS, 404, 399
Bower R. G., Benson A. J., Malbon R., Helly J. C., Frenk C. S., Baugh C. M., Cole S., Lacey C. G., 2006, MNRAS, 370, 645
Cantalupo S., Lilly S. J., Haehnelt M. G., 2012, MNRAS, 425, 1992
Capak P. L. et al., 2011, Nat, 470, 233
Cappelluti N., Ajello M., Burlon D., Krumpe M., Miyaji T., Bonoli S., Greiner J., 2010, ApJ, 716, L209
Carilli C. L. et al., 2004, AJ, 128, 997
Coil A. L. et al., 2009, ApJ, 701, 1484
Cole S., Kaiser N., 1989, MNRAS, 237, 1127
Cole S., Lacey C. G., Baugh C. M., Frenk C. S., 2000, MNRAS, 319, 168
Croom S. M. et al., 2005, MNRAS, 356, 415
Croton D. J. et al., 2006, MNRAS, 365, 11
De Lucia G., Blaizot J., 2007, MNRAS, 375, 2
DeGraf C., Di Matteo T., Khandai N., Croft R., Lopez J., Springel V., 2012, MNRAS, 424, 1892
Di Matteo T., Khandai N., DeGraf C., Feng Y., Croft R. A. C., Lopez J., Springel V., 2012, ApJ, 745, L29
Enoki M., Nagashima M., Gouda N., 2003, PASJ, 55, 133
Fan X. et al., 2003, AJ, 125, 1649
Fanidakis N., Baugh C. M., Benson A. J., Bower R. G., Cole S., Done C., Frenk C. S., 2011, MNRAS, 410, 53
Fanidakis N. et al., 2012, MNRAS, 419, 2797
Fanidakis N. et al., 2013, MNRAS, preprint (arXiv:1305.2200)
Francis P. J., Bland-Hawthorn J., 2004, MNRAS, 353, 301
Gilli R. et al., 2009, A&A, 494, 33
Gonzalez-Perez V., Lacey C. G., Baugh C. M., Frenk C. S., Wilkins S. M., 2013, MNRAS, 429, 1609
Guo Q., White S., Angulo R. E., Henriques B., Lemson G., Boylan-Kolchin M., Thomas P., Short C., 2013, MNRAS, 428, 1351
Häring N., Rix H.-W., 2004, ApJ, 604, L89
Husband K., Bremer M. N., Stanway E. R., Davies L. J. M., Lehnert M. D., Douglas L. S., 2013, MNRAS, 432, 2869
Kaiser N., 1984, ApJ, 284, L9
Kashikawa N., Kitayama T., Doi M., Misawa T., Komiyama Y., Ota K., 2007, ApJ, 663, 765
Kim H.-S., Baugh C. M., Benson A. J., Cole S., Frenk C. S., Lacey C. G., Power C., Schneider M., 2011, MNRAS, 414, 2367
Kim S. et al., 2009, ApJ, 695, 809
Komatsu E. et al., 2011, ApJS, 192, 18
Koutoulidis L., Plionis M., Georgantopoulos I., Fanidakis N., 2013, MNRAS, 428, 1382
Krumpe M., Miyaji T., Coil A. L., 2010, ApJ, 713, 558
Krumpe M., Miyaji T., Coil A. L., Aceves H., 2012, ApJ, 746, 1
Lacey C. G., Baugh C. M., Frenk C. S., Benson A. J., 2011, MNRAS, 412, 1828
Lagos C. D. P., Baugh C. M., Lacey C. G., Benson A. J., Kim H.-S., Power C., 2011, MNRAS, 418, 1649
Lagos C. d. P., Bayet E., Baugh C. M., Lacey C. G., Bell T., Fanidakis N., Geach J., 2012, MNRAS, 426, 2142
Mahadevan R., 1997, ApJ, 477, 585
Marulli F., Bonoli S., Branchini E., Moscardini L., Springel V., 2008, MNRAS, 385, 1846
Mo H. J., White S. D. M., 1996, MNRAS, 282, 347
Mortlock D. J. et al., 2011, Nat, 474, 616
Moster B. P., Somerville R. S., Maulbetsch C., van den Bosch F. C., Macciò A. V., Naab T., Oser L., 2010, ApJ, 710, 903
Moster B. P., Naab T., White S. D. M., 2013, MNRAS, 428, 3121
Mountrichas G., Georgakakis A., 2012, MNRAS, 420, 514
Narayan R., Yi I., 1994, ApJ, 428, L13
Norberg P. et al., 2001, MNRAS, 328, 64
Orsi A., Lacey C. G., Baugh C. M., Infante L., 2008, MNRAS, 391, 1589
Overzier R. A., Guo Q., Kauffmann G., De Lucia G., Bouwens R., Lemson G., 2009, MNRAS, 394, 577
Parkinson H., Cole S., Helly J., 2008, MNRAS, 383, 557
Porciani C., Magliocchetti M., Norberg P., 2004, MNRAS, 355, 1010
Priddey R. S., Ivison R. J., Isaak K. G., 2008, MNRAS, 383, 289

Ross N. P. et al., 2009, ApJ, 697, 1634
Shakura N. I., Sunyaev R. A., 1973, A&A, 24, 337
Shanks T., Croom S. M., Fine S., Ross N. P., Sawangwit U., 2011, MNRAS, 416, 650
Shen Y. et al., 2007, AJ, 133, 2222
Shen Y. et al., 2012, preprint (arXiv:1212.4526)
Sheth R. K., Tormen G., 1999, MNRAS, 308, 119
Springel V. et al., 2005, Nat, 435, 629
Starikova S. et al., 2011, ApJ, 741, 15
Stiavelli M. et al., 2005, ApJ, 622, L1
Swinbank J., Baker J., Barr J., Hook I., Bland-Hawthorn J., 2012, MNRAS, 422, 2980
Trainor R. F., Steidel C. C., 2012, ApJ, 752, 39
Trenti M., Santos M. R., Stiavelli M., 2008, ApJ, 687, 1
Wake D. A. et al., 2004, ApJ, 610, L85
Willott C. J., Percival W. J., McLure R. J., Crampton D., Hutchings J. B., Jarvis M. J., Sawicki M., Simard L., 2005, ApJ, 626, 657
Zehavi I. et al., 2005, ApJ, 630, 1
Zheng W. et al., 2006, ApJ, 640, 574

This paper has been typeset from a TEX/LATEX file prepared by the author.